Science of the Total Environment 912 (2024) 169349

Contents lists available at ScienceDirect

Science of the Total Environment

journal homepage: www.elsevier.com/locate/scitotenv

Environmental proteomics as a useful methodology for early-stage detection of stress in anammox engineered systems

Víctor Guzmán-Fierro [a], Alberto Dieguez-Seoane [b], Marlene Roeckel [a], Juan M. Lema [b], Alba Trueba-Santiso [b,*]

[a] Department of Chemical Engineering, Faculty of Engineering, University of Concepción, Concepción, Chile
[b] CRETUS, Department of Chemical Engineering, University of Santiago de Compostela, Campus Vida, Santiago de Compostela, Galicia, Spain

HIGHLIGHTS

- Anammox stress was detectable after only 28 h of exposure to copper.
- Stress proteins were overexpressed.
- Polysaccharide-biosynthesis protein and alginate exporter revealed higher EPS production.
- The presented workflow can be used for studying other metals or contaminants effects.
- Environmental proteomics can assess the treatability of industrial effluents.

GRAPHICAL ABSTRACT

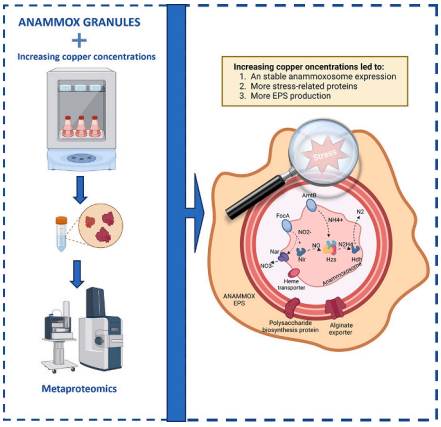

ARTICLE INFO

Editor: Damia Barcelo

Keywords:
Anammox process
Industrial effluents
Nitrogen removal
Proteomics
Stress-monitoring
Wastewater treatability

ABSTRACT

Anammox bacteria are widely applied worldwide for denitrification of urban wastewater. Differently, their application in the case of industrial effluents has been more limited. Those frequently present high loads of contaminants, demanding an individual evaluation of their treatability by anammox technologies. Bioreactors setting up and recovery after contaminants-derived perturbations are slow. Also, toxicity is frequently not acute but cumulative, which causes negative macroscopic effects to appear only after medium or long-term operations. All these particularities lead to relevant economic and time losses. We hypothesized that contaminants cause changes at anammox proteome level before perturbations in the engineered systems are detectable by macroscopic analyses. In this study, we explored the usefulness of short-batch tests combined with environmental proteomics for the early detection of those changes. Copper was used as a model of stressor contaminant, and anammox granules were exposed to increasing copper concentrations including previously reported IC_{50} values. The proteomic results revealed that specific anammox proteins involved in stress response (bacterioferritin, universal stress protein, or superoxide dismutase) were overexpressed in as short a time as 28 h at the higher

* Corresponding author at: CRETUS, Department of Chemical Engineering, University of Santiago de Compostela, Campus Vida, 15782 Santiago de Compostela, Galicia, Spain.
E-mail address: albamaria.trueba@usc.es (A. Trueba-Santiso).

https://doi.org/10.1016/j.scitotenv.2023.169349
Received 15 September 2023; Received in revised form 11 December 2023; Accepted 11 December 2023
Available online 15 December 2023

copper concentrations. Consequently, EPS production was also increased, as indicated by the alginate export family protein, polysaccharide biosynthesis protein, and sulfotransferase increased expression. The described workflow can be applied to detect early-stage stress biomarkers of the negative effect of other metals, organics, or even changes in physical-chemical parameters such as pH or temperature on anammox-engineered systems. On an industrial level, it can be of great value for decision-making, especially before dealing with new effluents on facilities, deriving important economic and time savings.

1. Introduction

Anaerobic ammonium oxidizing bacteria (anammox) are chemolithotrophs that gain their energy for growth from the anaerobic oxidation of ammonium, using nitrite as an electron acceptor to produce N_2 (Kuenen, 2008; Kartal et al., 2011). In nature, anammox is estimated to contribute up to 50 % of the nitrogen in the global air (Kartal et al., 2012; Kartal et al., 2013). These bacteria have been ubiquitously detected in anoxic environments where nitrogen compounds are degraded, and besides their biogeochemical and ecological relevance, they have also been applied worldwide in engineered systems for urban wastewater denitrification (WWTPs) (Kuenen, 2008). Anammox technology has lower oxygen and carbon source demand, as well as lower biomass production and greenhouse gas emissions when compared to conventional systems (Ren et al., 2020). It represents a clean and cost-effective solution for biological denitrification processes in line with the Sustainable Development Goals 6, 11, and 13 from the United Nations (United Nations, 2015).

Anammox bacteria are red-colored, due to their high content of cytochromes (Kartal et al., 2013) and their key nitrogen transformations occur inside an intracellular organelle, named anammoxosome which makes their cell architecture unique (Kartal et al., 2012). Additionally, anammox can grow on granules (i.e., self-aggregated biofilms) by producing extracellular polymeric substances (EPS) in which the cells are embedded (Kartal et al., 2012). In advanced WWTPs, operational parameters are optimized to favor this granulation that improves the settling velocity and biomass retention (Strous et al., 1998; Zhang et al., 2015; More et al., 2014). Anammoxosome enzymes rely on copper, iron, and molybdenum as cofactors (Reimann et al., 2015), and therefore metals, as well as ammonium and nitrite, should trespass the complex mixture of proteins, nucleic acids, phospholipids, humic substances, polysaccharides, and intercellular polymers that form the EPS (More et al., 2014) to reach the catalytic units.

To date, the application of a one-stage nitritation/anammox process to industrial wastewater has been more limited, when compared to urban waters. Yet, a few reports in the literature documented successful or explorative applications with different effluents (landfill leachate, monosodium glutamate wastewater, piggery wastewater, etc.) in different types of bioreactors including sequencing batch reactor, fluidized-bed, fixed-bed, up-flow anaerobic sludge bed or membrane bioreactors (Ren et al., 2022; Li et al., 2018a, 2018b). The main hindrance to the practical application of anammox technologies relies on their slow setting up (in the range of months) due to the observed long doubling times (15–30 days) and low specific growth rates (Kartal et al., 2012; Reino et al., 2018) of these bacteria, making the recovery after perturbations such as those derived from the presence of contaminants also very slow.

Nitrogen-rich industrial wastewater, such as those where the nitritation-anammox process is feasible frequently contains high loads of contaminants, including formaldehyde, pharmaceuticals, or heavy metals that can affect the performance of these microorganisms. Most of the previous research efforts focused on the macroscopic negative effects of pollutants on the anammox performance (removal rates) or settling characteristics (granules diameter) (Yang et al., 2013; Li et al., 2015; Zhang et al., 2016). Frequently, toxicity is not acute but cumulative, and inhibition takes place in the medium or long term. Therefore, acute toxicity tests do not anticipate those perturbations and long-term experiments are money and time-consuming. Taking all into consideration it is relevant to explore faster alternatives to evaluate the feasibility of anammox technologies to treat new specific wastewater. The authors hypothesized that molecular changes that occur in the cells before the decrease in the activity are detectable by conventional physical-chemical analyses, and before the system is destabilized. Consequently, it is of interest to find a suitable detection methodology and to identify biomarkers of early-stage stress.

Environmental proteomics is an umbrella term for a set of molecular techniques that allow the identification of the proteins being expressed by a mixed microbial community at a specific moment (Zhang et al., 2013). They have been increasingly applied to the study of microbiomes involved in biotechnological processes proving to be successful in detecting specific metabolic changes in highly complex communities (Quiton-Tapia et al., 2023) or confirming the biodegradation of specific pollutants (Kennes-Veiga et al., 2022; Poulsen et al., 2023). For instance, Wang et al. (2021) detected a reduction in the expression of key proteins from Ca. Brocadia nitrogen and carbohydrate metabolism during rapid temperature drops affecting the performance of a granular anammox reactor.

Although copper (Cu) is essential for cell metabolism, excessive concentrations are known to cause microbial inhibition negatively affecting macroscopic parameters such as nitrogen removal rates (NRR), or specific anammox activity (SAA) as it has been well reflected in the literature (Madeira and De Araújo, 2021). Yang et al. (2013), observed a significant decrease of SAA (94 %) at a copper concentration of 5 mg L^{-1}, resulting in 0.022 g N g VSS^{-1} d^{-1} and cell lysis. Their work concluded that the influent copper level should not be higher than 4 mg L^{-1} to maintain a good performance in long-term continuous-flow systems (Yang et al., 2013). In a similar range, 5 mg L^{-1} of copper nanoparticles reduced anammox NRR by 85 % after one month of incubation in Zhang et al. (2018). Different researchers determined median inhibitor concentrations (IC_{50}) in the range of 5 mg Cu^{2+} L^{-1} in anammox granular sludge (Aktan et al., 2021; Li et al., 2015). However, industrial wastewaters can present a wide variety of Cu concentrations: from pharmaceutical effluents, swine, or steel manufacturing wastewaters with 0–33 mg Cu^{2+} L^{-1} to mine waters within the range of g Cu^{2+} L^{-1} (Li et al., 2018a, 2018b).

The present study aimed to investigate the usefulness of a combination of short batch tests with anammox granules and environmental proteomics to detect early-stage anammox stress indicators. We used as an example of a potential stressor a heavy metal, copper, in concentrations between 0.1 and 5 mg L^{-1}. This early detection workflow can be of great value, especially to be implemented on facilities as a treatability test before dealing with new industrial wastewater.

2. Materials and methods

2.1. Granular sludge from anammox reactor

The anammox granules were collected from a pilot plant of 200 L consisting of a single unit, in the ELAN® process developed by the company FCC Aqualia in collaboration with the University of Santiago de Compostela. The influent of the pilot consists of rejected water from the anaerobic sludge digester of the urban WWTP located in Guillarei (Galicia, Spain) containing 540–1045 mg NH_4^+-N L^{-1} and operated at 30 °C (Val del Río et al., 2017).

2.2. Batch tests

The tests were carried out in 105 mL serum vials containing 63 mL synthetic wastewater. Each assay utilized a final concentration of 0.5 g VSS L^{-1} of anammox granular sludge. The mineral medium contained: $KHCO_3$, KH_2PO_4, $MgSO_4$ H_2O, $CaCl_2{\cdot}2H_2O$, and trace element solutions I (EDTA 2 Na_2H_2O and $FeSO_4$ $7H_2O$) and II (EDTA*$2Na_2H_2O$, $ZnSO_4$ $7H_2O$, $CoCl_2$ $7H_2O$, $MnCl_2$ $4H_2O$, $NaMoO_4$ $2H_2O$, $NiCl_2$ $6H_2O$, Na_2SeO_4 and H_3BO_3), as described by Van de Graaf et al. (1996). The initial concentrations of NH_4^+-N and NO_2-N were 100 mg L-1. The trace element solutions were prepared without copper that was then added as $CuSO_4$ $5H_2O$ in concentrations of: 0.1, 0.5, and 5 mg L-1 of Cu^{2+}. Controls without any copper were included. Four replicate microcosms were set up for each treatment (i.e.: copper concentration).

The bottles were then placed in a thermostatic shaker at 150 rpm. The temperature was maintained at 32 ± 1 °C and pH was adjusted to 7.0 by adding HCl solution to the medium. Samples were obtained over a period of 28 h using a syringe needle to analyze the concentrations of NH_4^+-N, NO_2-N, and NO_3-N. Ammonium (NH_4^+), nitrite (NO_2), pH, total suspended solids (TSS), and volatile suspended solids (VSS) were quantified according to the APHA Standard Methods (APHA, AWWA, WEF, 2012). The NRR was calculated by considering the production of nitrogen gas based on the stoichiometry described by Strous et al. (1998). This calculation involved the consumption of ammonia and nitrite as reactants. Additionally, the SAA was calculated by normalizing the nitrogen removal at each time point with respect to the sludge concentration in the assay (Dapena-Mora et al., 2007). Statistical analyses were performed using analysis of variance (ANOVA) with Tukey's test as a post hoc analysis with GraphPad Prism version 5.0 (GraphPad Software, USA). P values <0.05 were considered statistically significant.

2.3. Proteome extraction

After each assay, 10 mL was collected at the final incubation time (28 h) and centrifuged at 6000 rpm for 10 min. First, triplicate fractions of 150 mg of wet pellet were washed with PBS [137 mM NaCl, 2.7 mM KCl, 10 mM Na_2HPO_4, 1.8 mM KH_2PO_4, pH 7.4] and then resuspended with extraction buffer [50 mM Tri's buffer, 1 % SDS (Aplichem Panreac, USA), pH 7.5]. Cell disruption was performed by sonication with an ultrasonic cell disruptor (Branson Sonifier S-150, USA) on ice at a maximum of 40 % energy with an output power of 0.08 watts RMS for three cycles of 1 min to break aggregates and lyse the cells. After this, the samples were centrifuged (Eppendorf centrifuge 5417R, Eppendorf, Germany) for 20 min at 3700 ×g at 4 °C. Finally, the supernatant was collected. To concentrate the proteins and to clean them from buffers, salts, or organic contaminants at least two steps of 10 % trichloroacetic acid (TCA, Sigma Aldrich) at 4 °C precipitation were done. Then, the tubes were centrifuged (10 min, 9000 ×g, 4 °C) (Universal 320, Hettich, Germany), the supernatant was discarded, and the obtained pellet was resuspended in 100 mM triethylammonium bicarbonate (TEAB) buffer, pH 8.5 (Sigma-Aldrich, Spain). Protein quantification was done with the Pierce™ bicinchoninic acid assay (BCA) Protein Assay Kit (ThermoFisher Scientific, USA), using a bovine serum albumin (BSA) standard curve. Triplicate independent extractions were performed from each microcosm and then all samples belonging to each copper treatment were pooled together before further proteomic analyses. The values presented here are the average and the standard concentrations of the three individual extracts for each treatment before their pooling.

2.4. SDS-PAGE electrophoresis

To check the similarity of replicates and the quality of the samples (i.e., protein degradation), sodium dodecyl sulfate-polyacrylamide gel electrophoresis in denaturing conditions (SDS-PAGE) was performed, following the procedure detailed in Kennes-Veiga et al., 2022. Briefly, electrophoresis was run for duplicate aliquots with 10 μg protein/well. Protein samples were mixed with NuPAGE LDS Sample Buffer and NuPAGE Reducing Agent according to manufacturer instructions. As a molecular weight marker, the PageRuler™ Plus Prestained Ladder from 10 to 250 kDa (ThermoFisher Scientific, USA) was included. Bis-Tris NuPAGE 4–12 % gel was used (ThermoFisher Scientific, USA) and electrophoresis was run at 200 V. Protein bands were visualized using the Imperial™ Protein Stain (ThermoFisher Scientific, USA) following the manufacturer's protocol.

2.5. Protein analysis by mass spectrometry

A label-free approach was used for the quantification of the proteins present in each sample (Zhang et al., 2013). First, samples were trypsin-digested, reduced-alkylated, and finally desalted using ZipTip-μC18 material (Merck, Germany). The obtained peptide samples were analyzed by in-solution shotgun proteomics (Zhang et al., 2013). Peptide samples (0.2 μg of protein) were injected onto a timsTOF Pro mass spectrometer (Bruker, Bremen, Germany) equipped with a nano-electrospray source (CaptiveSpray) and a tims-QTOF analyzer. The chromatographic analysis was performed using a nanoELUTE chromatograph (Bruker) with an Aurora analytical column (C18, 250 × 0.075 mm, 1.6 μm, 120 Å, IonOpticks). The nHPLC was configured with binary mobile phases that included solvent A (0.1 % formic acid in miliQ H_2O) and solvent B (0.1 % formic acid in acetonitrile). The analysis time was 105 min, in which the B/A solvent ratio was gradually increased. Blanks were injected between samples with an analysis time of 60 min, confirming no carry-over. For mass spectrometry (MS) acquisition, a collision-induced dissociation (CID) fragmentation and a nanoESI positive ionization mode was employed. PASEF-MSMS scan mode was established for an acquisition range of 100–1700 m/z (Quiton-Tapia et al., 2023). Matches were filtered for 1 % false discovery rate (FDR) at the peptide level. MS analyses were performed at the Mass Spectrometry and Proteomics Unit (Area of Infrastructures) of the University of Santiago de Compostela.

2.6. Metaproteomic data analysis

MS/MS spectra were processed with PEAKS Studio (Bioinformatics Solutions, Canada) software for protein identifications and quantifications based on the spectral counting method and the Spec value. Due to the nature of these samples (incompletely characterized from a genomic point of view) and the focus of this study, we used a homemade database (Zhang et al., 2013) with all protein sequences available in NCBI protein from the anammox genera *Brocadia, Jettenia and Kuenenia* (order Brocadiales). The Compare module from PEAKS Studio (software PEAK Studio 10.6, Bioinformatics Solutions Inc., Canada) was used for protein label-free quantification using the sample Control as control. The value Spec presented here is the result of this comparison. MS data was processed in Protein Group mode. The mass spectrometry proteomics data was deposited in the ProteomeXchange Consortium via the PRIDE partner repository with the dataset identifier PXD041756. As first stringent filtering, the first protein of each protein group was manually selected, and the others were not considered. Also, only those proteins identified with at least 2 unique peptides were considered in this study (Zhao and Lin, 2010). Graphs were made using GraphPad Prism v8.0 (GraphPad Software, USA). The values on the heatmaps were normalized by the next expression: $Row_{norm} = (Row_i - Mean)/(Row_{max} - Row_{min})$. Where Row_i represents the row of the group containing protein i for each copper concentration. Row_{min} and Row_{max} denote the minimum and maximum values, respectively, of the group for each copper concentration (Galili et al., 2018). If $Row_{min} = Row_{max}$, $Row_{norm} = 0$. For the Venn diagram, the software VENNY 2.1 was used (Oliveros, 2007-2015). GO categorization and treeview visualization of Ca. Brocadiaceae relative abundances was done in Unipept Desktop v.3.0. (Mesuere et al., 2015).

2.7. Basic local alignment search tool analysis (BLAST)

BLAST analysis was used after the proteomic pipeline to find homologous for those proteins annotated as "hypothetical proteins". The BLAST tool available at the NCBI website was used to compare the listed proteins against those included in the database of "Candidatus Brocadiales" (NCBI taxid:1127829). Significant similarity was considered when the obtained *E*-values were below 1×10^{-20} (Boleij et al., 2020).

3. Results and discussion

3.1. Effect of copper concentrations on anammox activity

NRR of anammox granules at different copper concentrations was measured after an incubation period of 28 h (Fig. 1). >83 % of the nitrogen was consumed in all assays. The mean SAA of the control and the test conducted with 5 mg L^{-1} was 0.25 g N g VSS^{-1} d^{-1}, and no significant difference was observed between the SAA values (*p*-value = 0.5087, 95 % confidence interval). It has been previously reported that in longer incubations similar copper concentrations led to decreased anammox activities. For instance, Yang et al. (2013) observed a significant decrease in SAA (94 %), resulting in 0.022 g N g VSS^{-1} d^{-1} and cell lysis. Zhang et al., 2018 detected a reduction of anammox NRR 85 % after one month of incubation with copper nanoparticles and Aktan et al. (2021) determined an IC_{50} of 6.7 mg L^{-1} in long-term (6.74 mg L^{-1}) experiments (240 days). We therefore predict that a longer incubation might have led to reduced anammox activities.

3.2. Anammox community composition

Proteome samples were collected after 28 h of incubations, extracted, and analyzed by environmental proteomics. The protein concentration (μg protein/μL) determined by BCA on the triplicate proteome samples from each treatment were 1.45 ± 0.01 (0.1), 1.69 ± 0.02 (0.5), 1.36 ± 0.01 (5), 1.65 ± 0.01 (0, Control), respectively. The results presented from here on correspond to the combination of 3 individual extracts. As quality control of the proteome samples, an SDS-PAGE electrophoresis was performed confirming the absence of protein degradation and a good representation of proteins from all the protein sizes in all cases (Fig. S1). The number of proteins identified ranges from 3996 (0.5 mg Cu L^{-1}) to 5015 (control). The structure of the anammox population was assessed in all the copper concentrations by calculating the relative contribution of peptides belonging to each genus with respect to the total of peptides identified on each sample (Blakeley-Ruiz and Kleiner, 2022; Kennes-Veiga et al., 2022) (Fig. 2A). Ca. Brocadia was the predominant genus with a 92 ± 0.2 % relative abundance, while a minor presence of Ca. Jettenia (7.1 ± 0.2 %) and Ca. Kuenenia (1.3 % ± 0.1) was detected in all cases. Therefore, the copper concentrations applied in this study (0–5 mg Cu L^{-1}) did not have an impact on the abundance of any of the anammox genera as expected considering the relatively long doubling times of anammox bacteria (e.g., 7–11 days) (Kartal et al., 2012) and the short incubation time applied in the present study.

In all the cases, Ca. Brocadia fulgida was the predominant species from the genus (90.2 % ± 0.7 %) (Fig. 2B). Our proteomic results match with previous studies showing by metagenomic techniques that Ca. Brocadia fulgida is the predominant microorganism in anammox sludge from the same WWTP used in this study, with relative abundances ranging from 80 % to 90 % (Morales et al., 2015).

3.3. Proteome identifications

A Venn diagram was created to display the number of common and unique protein identifications across different treatments after selecting only those proteins identified with at least 2 unique peptides (Zhao and Lin, 2010) (Fig. 3). The diagram revealed that 352 (53.3 %) proteins were shared across all samples. The samples with 0 (control) and 5 mg L^{-1} of copper showed the highest number of unique proteins in the analysis, at 8.2 % and 7 %, respectively. In the Venn diagram, the unique proteins for each treatment are categorized according to GO molecular function. The unique proteins detected on the 5 mg Cu L^{-1} treatment mainly belong to the category's metabolic pathways and bacterial metabolism in diverse environments is more abundant. It is also worth to mention the appearance of proteins from the two-component system.

3.4. Gene ontology (GO) protein categories had a differential expression influenced by copper concentration

Regarding the subcellular location of the proteins detected on the metaproteomic analyses, most of them belong to the membrane fraction (42 %), followed by the cytoplasm (22 %), plasma membrane (13 %), ribosome (7 %) and anammoxosome (5 %) (Fig. 4). Anammox cell architecture is peculiar as these bacteria harbor a triple-layered membrane: periplasmic, cytoplasmic, and a specialized membrane enveloping the anammoxosome (De Almeida et al., 2016). This sophisticated arrangement and the corresponding membrane-bound proteins

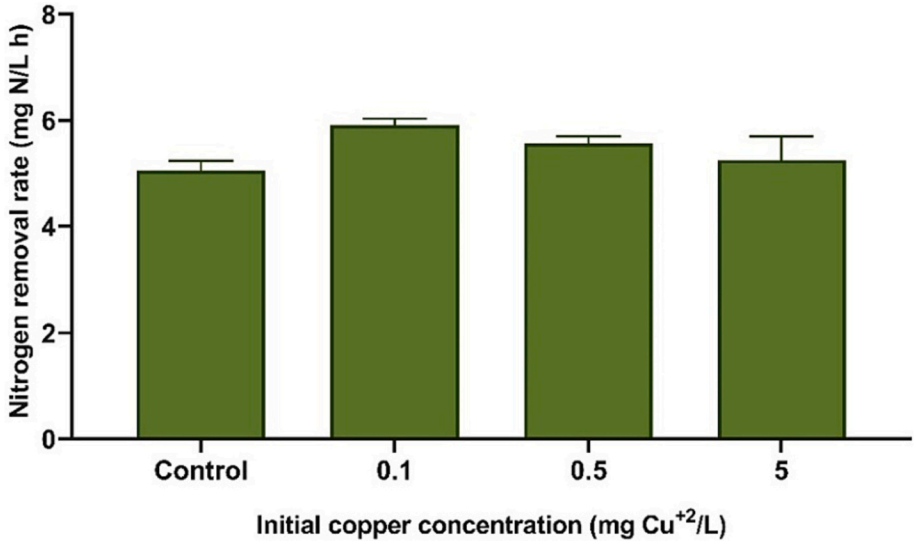

Fig. 1. Nitrogen removal rate of anammox granules exposed to increasing copper concentrations after 28 h of exposure.

A)

Genus	Copper concentration (mg Cu^{+2}/L)			
	Control	0.1	0.5	5
Brocadia	91.3%	91.7%	91.7%	91.7%
Jettenia	7.3%	7.1%	6.8%	7.0%
Kuenenia	1.4%	1.2%	1.5%	1.3%

B)

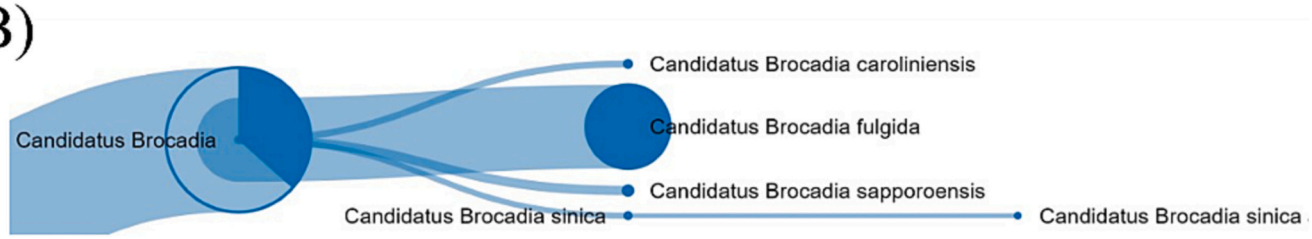

Fig. 2. A: Relative abundance of each anammox genera in the proteomes from each Cu treatment. B: Treeview visualization (Mesuere et al., 2015) of the relative abundance of Ca. *Brccadia* members at 5 mg Cu^{2+}/L.

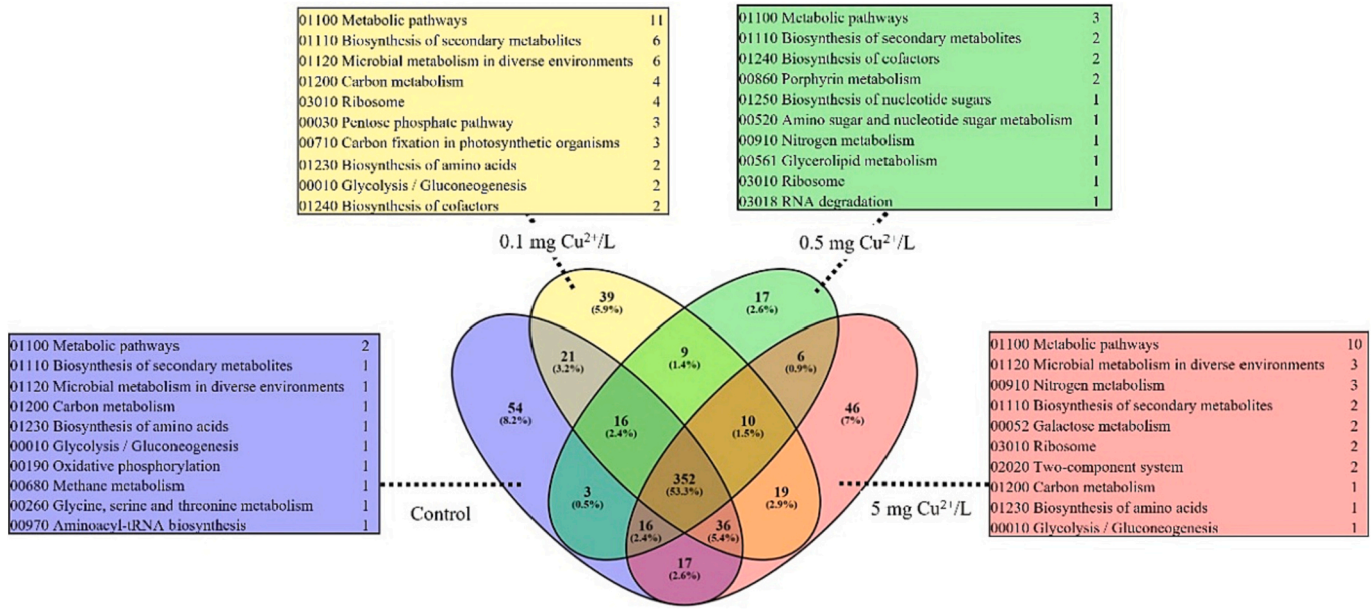

Fig. 3. Venn diagram showing the number of proteins identified in Anammox sludge after incubation with different copper concentrations. The intersection of ellipses indicates the number of proteins shared between samples.

play a crucial role in the efficiency of their respiratory processes. Among treatments, we detected a differential expression of membrane fraction, cytoplasm, and ribosome more represented in the assays Control and 0.1 mg Cu L^{-1}. On the other hand, the expression of plasma membrane and extracellular proteins was increased in the higher copper concentration (5 mg Cu L^{-1}). The anammoxosome exhibited consistent expression levels across all copper assays (Fig. 4). The anammoxosome constitutes the heart of the anammox catabolism being so far, a unique cell organelle that allocates the three main enzymes for ammonia and nitrite anaerobic oxidation. The periplasm contains the most numerous and diverse copper-dependent enzymes in bacteria. Accordingly, this compartment is most at risk of copper-induced damage, which is exacerbated under anoxic conditions (Zhang et al., 2017).

Considering the molecular function classification, metal ion binding was the most abundant category (17 %), followed by ATP binding (12 %), oxidoreductase activity (8 %), heme binding (7 %), and electron transfer activity (7 %) (Fig. S2). This is indicative of the anammox dependence on the metals present in the environment and redox reactions. Metal ion binding proteins are strongly associated with electron transfer or redox catalysis, essential in anammox energy metabolism (Ferousi et al., 2019). Extracellular proteins from anammox granules have been observed to exhibit a faster response in binding Cu^{2+} than polysaccharides and hydrocarbons, with carboxyl groups playing a significant role. (Li et al., 2020). A recent study investigated the multimetal adsorption capacity of EPS protein from anammox granular sludge and found that the adsorption capacity for copper was highly dependent on the extracellular matrix (Pagliaccia et al., 2022).

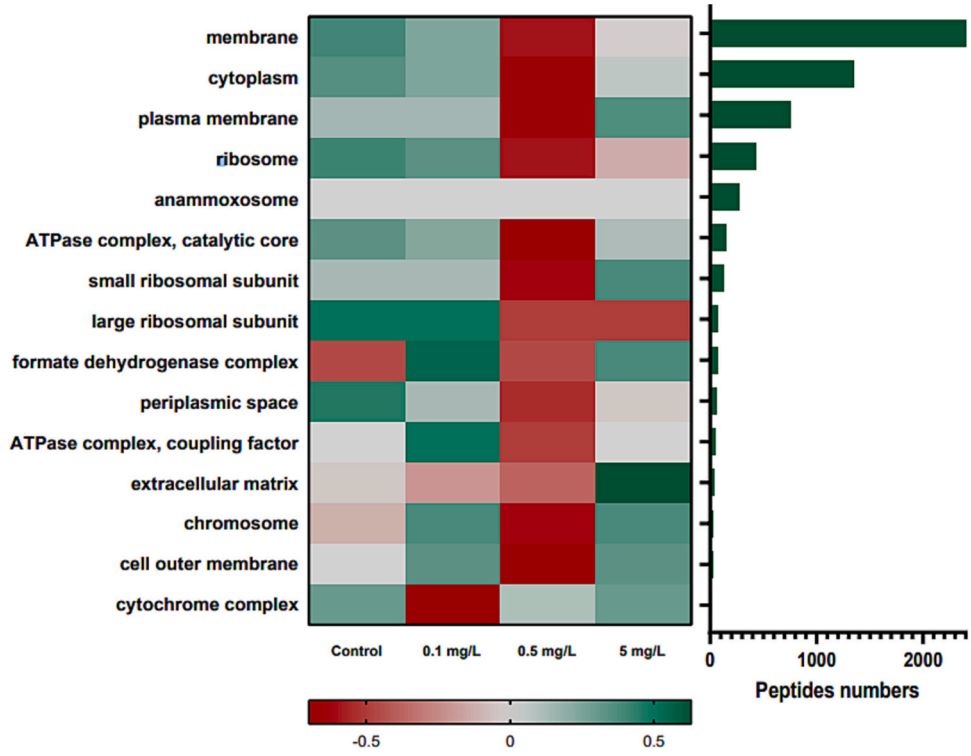

Fig. 4. Heatmap representing the Gene Ontology (GO) classification of the proteins detected in the anammox sludge after 28 h in the presence of the different copper concentrations applied, according to the categories of Cellular components. The corresponding number of total peptides identified for each category accompanies each heatmap on the right Y axis.

3.5. Nitrogen metabolism

Those proteins known to be involved in anammox nitrogen metabolism were specifically searched for in this study. The results are detailed here following the same track as a nitrite and ammonium molecule would follow. First, the nitrite transporter (FocA) and the ammonium transporter (AmtB) are localized on the anammoxosome membrane and are responsible for importing the nitrogen species into the core anammox energy machinery. This distinctive cellular structure, termed the anammoxosome, contains three enzymes acting in the following order: i) nitrite reductase (Nir), which converts nitrite into nitric oxide (NO), ii) hydrazine synthase (Hzs), which combines NO and ammonium to form the singular intermediate compound hydrazine (N_2H_4) and iii) hydrazine dehydrogenase (Hdh), forming dinitrogen gas from hydrazine (Kartal and Keltjens, 2016).

In all the proteomes analyzed, the nitrite transporter FocA (KKO18363.1) and the nitrite reductases from *B. fulgida* were detected among the 4–6 most abundant proteins in all samples (Table 1). The ammonium transport protein (AmtB, RIK00381.1), localized on the anammoxosome membrane was also detected in all samples (although in different ranking positions).

Hydrazine synthase (Hzs) is responsible for the so-called anammox reaction: the conversion of ammonium and nitric oxide or hydroxylamine to produce the toxic hydrazine. Hzs is a unique enzyme from anammox, considered a biochemical novelty, and its function cannot be replaced by other proteins, making his gene an appropriate functional biomarker for the detection of these bacteria by PCR (Yang et al., 2018). This enzyme is an heterotrimer, encoded by the hzsCBA gene cluster, and in our proteome samples, HzsA (AEW50030.1) and HzsC (KKO20885.1) from Ca. Brocadia fulgida were always among the three most abundant proteins (Tables S1-S4), indicating the extreme degree of specialization of anammox cells on this energy metabolism.

Hydrazine dehydrogenases (Hdh) (KKO18553.1) were expressed in all samples. This homotrimetic enzyme catalyzes hydrazine oxidation and therefore produces about half of all N_2 emitted into the atmosphere (Kartal et al., 2012). Hdh are iron-dependent and belong to the HAO-like octaheme proteins being therefore related to the hydroxylamine oxidoreductase (HAO) from aerobic ammonium-oxidizing bacteria (De Almeida et al., 2016; Kartal et al., 2011) and in the public genome of Ca. Brocadia fulgida they are annotated as HAO. The expression of the individual proteins from the anammoxosome was not affected by the copper concentration, as pointed out in the GO analysis detailed in Section 3.4. This is different to what described in the case of temperature stress in Wang et al., 2021, where Hzs was significantly less expressed after a temperature drop from 35 °C to °15 °C. Also, the presence of high concentrations of organic compounds such as p-nitrophenols has been shown to decrease the expression of expression of Hzs and other

Table 1
Anammox proteins involved in the nitrogen metabolism detected in the present study by metaproteomics and their Spec value at the end of the experiments in the different copper treatments. The Spec value is based on peptide spectrum matches (PSM) and was used as an indicator for the relative abundance of the proteins in each sample.

Nitrogen metabolism					
Protein	Accession	Control	0.1	0.5	5
Nitrite transporter - FocA	KKO18363.1	8	4	0	7
Ammonium transporter – AmtB	RIK00381.1	19	13	9	10
Nitrite reductase - Nir	OQZ00558.1	206	215	196	207
Nitrite reductase - Nir	KKO18751.1	186	150	108	123
Hydrazine synthase - HzsA	AEW50030.1	679	557	592	703
Hydrazine synthase - HzsB	BBO18371.1	35	29	37	32
Hydrazine synthase - HzsC	KKO20885.1	243	234	240	286
Hydrazine dehydrogenases - Hdh	KKO18553.1	116	100	83	100
Heme transporter CcmC	OQZ02497.1	291	261	254	299
Periplasmic nitrate (or nitrite) reductase - NapC_nirT	UJS19330.1	32	30	27	22

anammoxosome enzymes in Luo et al., 2022.

The heme transporter CcmC (OQZ02497.1) was also among the three most abundant proteins in all proteome samples. Heme c is a very important co-factor in the main anammox metabolic reactions with catalytic and electron-transfer potential and is responsible for the characteristic carmin color on enriched anammox biomass. Ma et al. (2019) showed how heme C concentration measured by a spectrophotometry-dedicated method was positively correlated with NRR in anammox cultures and therefore also a possible indicator to evaluate anammox performance. In our study, the abundance of this iron-dependent cytochrome did not show a trend related to the presence of copper (Table 2) pointing to a general good fitness on the anammox energy system. These results also demonstrate that the use of metaproteomics to detect anammox-specific activities in engineered systems is technically possible.

Interestingly, we also detected a protein annotated as '*napC_nirT periplasmic nitrate (or nitrite) reductase c-type cytochrome*' (UJS19330.1). According to the NCBI, nearly every member of this subfamily is a nitrate reductase, specifically NapC. This is a predicted membrane-anchored four-heme c-type cytochrome that forms one component of the periplasmic nitrate reductase along with other Nap*ABDEF subunits. A single known exception currently is NirT, which is a component of a nitrite reductase. To elucidate the implication of this expressed enzyme on nitrite or nitrate reduction would require further research effort.

3.6. Anammox central carbon metabolism

The central carbon metabolism of anammox was resolved by Lawson et al. (2021) using carbon and hydrogen isotope tracing and metabolomics. Anammox are not able to use acetate as carbon or energy source in situ and these bacteria make use of the Wood Ljungdahl/acetyl-coenzyme A (CoA) pathway for carbon fixation. In this pathway, high-energy electrons from hydrazine are transferred via ferredoxin to the acetyl-CoA synthetase/CO dehydrogenase, and the replenishment of the hydrazine pool to compensate the investment in carbon fixation is achieved by reverse electron transport. The activity of the oxidative branch of the tricarboxylic acid cycle for alpha-ketoglutarate biosynthesis and the direct assimilation of extracellular formate via the Wood-Ljungdahl pathway instead of its complete oxidation to CO_2 followed by reassimilation was confirmed.

Even though no carbon source was added to the medium in the present study we detected the following enzymes from the Wood Ljungdahl pathway: CO dehydrogenase/acetyl-CoA synthase (KKO18855.1), alcohol dehydrogenase (RIJ91218.1), methyltransferase (RIJ92330.1), methylene-H4F-dehydrogenase (OQY97878.1), formyl-H4F synthase (KKO19470.1) and formate dehydrogenase (OQY98926.1). No enzyme from the TCA cycle was found expressed and from the gluconeogenesis, the phosphoglycerate kinase (UJS20358.1), fructose-1,6-bisphosphatase (UJS19600.1), and glucose-6-phosphatase.

Table 2
Selected anammox proteins related to stress and EPS production identified by shotgun metaproteomics in this study that showed an increased expression in response to the increasing copper concentrations. The Spec value for each protein on each copper treatment concentration (mg L^{-1}) is shown. The colors are indicative of the abundance, from red (less abundant) to green (most abundant).

Stress-related proteins					
Protein	Accession	Control	0.1	0.5	5
Universal stress protein	KKO18817.1	21	20	18	26
Bacterioferritin	RIJ99420.1	11	19	16	25
Superoxide dismutase	OQY97949.1	47	36	36	54
Multicopper oxidase domain-containing protein	UJS22045.1	0	4	9	15
RNA-metabolising metallo-beta-lactamase	KKO20060.1	8	10	17	23
EPS Production					
Protein	Accession	Control	0.1	0.5	5
Alginate export family protein - AlgE	KKO20581.1	212	211	253	331
Alginate export family protein - AlgE	WP_052562998.1	79	104	115	114
Polysaccharide biosynthesis protein	UJS22320.1	0	0	3	6
Sulfotransferase	UJS22315.1	0	0	0	3

3.7. Stress response

Despite the homogeneous NRR found in the different copper treatments and the stable expression of the anammoxosome, we detected an increase in the expression of specific proteins previously linked to stress conditions. The abundance of the protein annotated as '*Multicopper oxidase domain-containing protein*' from Ca. Brocadia sp. (UJS22045.1.) increased in a manner directly proportional to the copper concentration (Fig. 5). The link between this protein and the general mechanism to protect cells against the toxicity of the copper accumulated in the periplasm has been previously well-described in clinical bacteria such as *E. coli* or *Mycobacterium tuberculosis* (Ladomersky and Petris, 2015).

Other stress-related proteins, such as bacterioferritin, universal stress protein, or superoxide dismutase showed the highest expression on the highest copper concentration (5 mg L^{-1}), yet they did not follow such a clear trend as the two previously discussed (Table 2). Additional proteins related to stress in anammox cells in Zorz et al. (2018), i.e., specific chaperones, transporters, ATPases, alkyl hydroperoxide reductase, ruberyhtrin family-protein and B12-binding domain-containing radical SAM protein were present in our samples, yet not differentially expressed in regards of the copper treatment (Table S1-S4).

Unexpectedly, we also detected an increased expression of the 'RNA-metabolising metallo-beta-lactamase (MBL)' (KKO20060.1) in response to copper (Fig. 5). We did not add any β-lactams in our microcosms and, even when anammox granules were collected from a WWTP treating urban wastewater, they were washed before protein extraction. It is, therefore, improbable the presence of antibiotics in the experiments and their activity might be different than β-lactamase. Blasting of its full aminoacidic sequence in NCBI gives the highest identities with other 'MBL fold metallo-hydrolases' both from the genus Ca. Brocadia. Interestingly, these enzymes were recently found to have promiscuous activities such as hydrolyzing a wide range of substrates, like DNA or RNA, apart from β-lactams and have been found in humans, archaea, fungi, and now viruses (Colson et al., 2020). This is different from the drastically simplified paradigm of enzymes with β-lactamase activity being expressed by bacteria derived from the selective pressure of natural or prescribed antibiotics (Colson et al., 2020).

The reason why its expression was related to the copper concentration is also not evident to us. MBL lactamases are dependent on periplasmic zinc ions to catalyze the hydrolysis of β-lactams. Zinc ions can be exchanged with cadmium, cobalt, and manganese maintaining catalytically active enzymes (Page and Badarau, 2008). However, Djoko et al. (2018) showed that copper ions inhibit the activity of MBL in vitro and enhance β-lactams susceptibility of *E. coli* isolates harboring MBL. It would therefore deserve more research effort to elucidate the anammox MBL activity and its interaction with copper in the conditions used in this study.

3.8. Specific proteins responsible for EPS production increased in the presence of copper

The proteins 'alginate export family protein' (AlgE) and 'polysaccharide biosynthesis protein' were detected only in the genus *Brocadia* and interestingly, their expression was augmented in those microcosms with supplemented copper (Table 2). Alginate is an exopolysaccharide known to be part of the sugar-based part of the EPS of anammox. Additionally, the protein annotated as 'sulfotransferase' (accession UJS22315.1) from Ca. Brocadia and linked to the synthesis of sulfated glycosaminoglycans (or glycoprotein) in anammox EPS (More

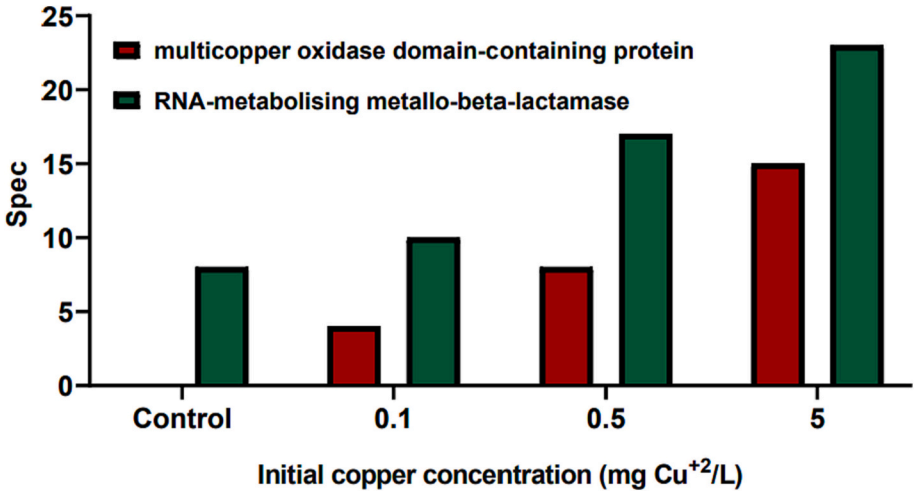

Fig. 5. Impact of copper concentration on the spectral peptide match counts of the 'multicopper oxidase domain-containing protein' (UJS22045.1) and the 'RNA-metabolising metallo-beta-lactamase' (KKO20060.1) from anammox granules.

et al., 2014) was detected only at the highest copper concentration applied (5 mg L^{-1}) with a Spec value of 3 (Table 2). Our results indicate a higher production of EPS from Ca. Brocadia in response to copper, as it was previously shown in other bacterial genera such as *Enterobacter aerogenes* or *Pseudomonas putida* (More et al., 2014) and for anammox granules in several studies (Zhang et al., 2015). Zhang et al. (2015) investigated the tolerance mechanism of granular anammox bacteria against copper by extracting the EPS and quantifying its total protein content by the Lowry method and found that higher copper concentrations trigger an increase in protein levels within the EPS, effectively shielding the anammox cells. In our study, we detected an increase in proteins located in the extracellular matrix and additionally, we have identified which specific proteins are increasing as an early-stage response to the presence of stressing concentrations of copper. Apart from this underlying mechanism of copper self-protection, it was proposed that anammox cells self-heal by actively pumping heavy metals out of the most sensitive regions of the cells, i.e., active efflux mechanisms (Zhang et al., 2016). We did not detect an increase in any of the efflux pumps or membrane transporters. Therefore, the results of our study point to the first mechanism as an early response to the presence of inhibitory copper concentrations in anammox granules.

An increase in anammox EPS production has also been demonstrated in response to other metals, such as nickel or cadmium (Zhang et al., 2023). Both are of great relevance for industrial facilities, as nickel is widely used in electroplating, catalysts, paints, and other fields, while cadmium is present in metal refinery discharges, waste batteries runoff or pesticides manufacturing waters among others. Similarly, salinity has been shown to increase the EPS production and alter the community structure of anammox systems in Wu et al., 2019. In the present context of a climatic crisis, salinity is a very relevant parameter to be considered. Other physical-chemical parameters that have been described to alter the microbial activities, and more specifically the proteome expressions in anammox are temperature or pH (Izadi et al., 2021). Also, organic compounds such as nitrophenols have been described to reduce the EPS content on anammox granules, altering the settling properties of their granules (Luo et al., 2022).

4. Conclusions

The increasing concentrations of the contaminant applied to the anammox granules led to interesting findings at the proteome level. First, in agreement with the macroscopic results (similar NRR), anammoxosome enzymes expressions were stable in all copper treatments. The hydrazine synthase is widely considered a molecular biomarker for anammox activity and was the most abundant enzyme in all proteomes. This fact proves that environmental proteomics can be applied to tracking this microbial activity in engineered systems. This is of interest as previous studies have shown impacts on the hydrazine synthase activity by temperature drops or the presence of organics such as nitrophenol. For the early detection of copper-derived stress, other proteins were found to be more useful. Specific anammox proteins related to stress and EPS production increased their abundance proportionally to copper concentration. Moreover, another group of stress-related proteins showed their highest expression at 5 mg Cu L^{-1}. The detected indications of anammox stress are in agreement with previous literature reports of copper IC_{50} values in the range of 5 mg Cu L^{-1}. Our results suggest that environmental proteomics is technically useful for detecting early-stage stress biomarkers in anammox bacteria. This methodology appears to provide more information regarding pollutants' effects on bacteria than targeted techniques, such as qPCR, that only detect specifically selected genes (e.g.: hydrazine synthase). The negative effect of copper on anammox proteomes was detectable after an exposure time as short as 28 h. and this suggests that the methodology described in this study can, therefore, be translated into relevant time and consequently economic savings in wastewater treatment facilities leading to industrial wastewater. The proposed approach would consist of testing the new effluents to be treated with this methodology before full-scale bioreactors are set up or loaded. The methodology applied here for the study of copper effects can be transferred to the study of the effect of other contaminants such as different heavy metals (including cadmium, nickel, and others), organics such as nitrophenol, or the volatile fatty acids present in high concentrations on the effluent of anaerobic digestors often subjected to anammox treatments. Also, changes in physical-chemical parameters such as temperature, pH, or salinity are expected to leave a proteomic trace, according to previous literature reports. This study also opens the door to exploring this methodology on other groups of bacteria relevant for wastewater treatment (e.g.: AOB, ammonia-oxidizing bacteria) or other biotechnological processes.

CRediT authorship contribution statement

Víctor Guzmán-Fierro: Formal analysis, Investigation, Writing – original draft, Writing – review & editing. **Alberto Dieguez-Seoane:** Investigation, Writing – review & editing. **Marlene Roeckel:** Conceptualization, Investigation, Project administration, Resources, Supervision, Writing – review & editing. **Juan M. Lema:** Conceptualization, Formal analysis, Project administration, Supervision, Validation, Writing – review & editing. **Alba Trueba-Santiso:** Conceptualization,

Data curation, Formal analysis, Investigation, Methodology, Project administration, Supervision, Validation, Visualization, Writing – original draft, Writing – review & editing.

Declaration of competing interest

The authors declare that they have no known competing financial interests or personal relationships that could have appeared to influence the work reported in this paper.

Data availability

Data will be made available on request.

Acknowledgments

In memory of Antonio Trueba de la Iglesia (Tio Comino). The authors thank FCC Aqualia for the partial nitritation-anammox ELAN® granular biomass samples provided that allowed them to perform this study. Marlene Roeckel and Víctor Guzmán-Fierro were supported by Agencia Nacional de Investigación y Desarrollo [1200583 (FONDECYT) and 2018-21180541]. Juan M. Lema Rodicio and Alba Trueba-Santiso belong to the Galician Competitive Research Group (GRC) ED431C-2021/37. Alba Trueba-Santiso acknowledges a Juan de la Cierva-Formación postdoctoral Grant (FJC2019-041664-I).

Appendix A. Supplementary data

Supplementary data to this article can be found online at https://doi.org/10.1016/j.scitotenv.2023.169349.

References

Aktan, C.K., Yapsakli, K., Mertoglu, B., 2021. Short- and long-term effects of copper on anammox under gradually increased copper concentrations. Biodegradation 32, 273–286. https://doi.org/10.1007/s10532-021-09934-1.

APHA, AWWA, WEF, 2012. Standard Methods for Examination of Water and Waste Water, 22nd edition. American Public Health Association, Washington DC.

Blakeley-Ruiz, J.A., Kleiner, M., 2022. Considerations for constructing a protein sequence database for metaproteomics. Comput. Struct. Biotechnol. J. 20, 937–952. https://doi.org/10.1016/j.csbj.2022.01.018.

Boleij, M., Kleikamp, H., Pabst, M., Neu, T.R., Van Loosdrecht, M.C.M., Lin, Y., 2020. Decorating the Anammox house: sialic acids and sulfated Glycosaminoglycans in the extracellular polymeric substances of Anammox granular sludge. Environ. Sci. Technol. 54 (8), 5218–5226. https://doi.org/10.1021/acs.est.9b07207.

Colson, P., Pinault, L., Azza, S., et al., 2020. A protein of the metallo-hydrolase/oxidoreductase superfamily with both beta-lactamase and ribonuclease activity is linked with translation in giant viruses. Sci. Rep. 10, 21685. https://doi.org/10.1038/s41598-020-78658-8.

Dapena-Mora, A., Fernández, I., Campos, J.L., Mosquera-Corral, A., Méndez, R., Jetten, M.S.M., 2007. Evaluation of activity and inhibition effects on the Anammox process by batch tests based on the nitrogen gas production. Enzym. Microb. Technol. 40 (4), 859–865. https://doi.org/10.1016/j.enzmictec.2006.06.018.

De Almeida, N.M., Wessels, Hans J.C.T., de Graaf, Rob M., Ferousi, Christina, Jetten, Mike S.M., Keltjens, Jan T., Kartal, Boran, 2016. Membrane-bound electron transport systems of an anammox bacterium: a complexome analysis. Biochim. Biophys. Acta (BBA) Bioenerg. 1857 (10), 1694–1704. https://doi.org/10.1016/j.bbabio.2016.07.006.

Djoko, K.Y., Achard, M.E.S., Phan, M.D., Lo, A.W., Miraula, M., Prombhul, S., et al., 2018. Copper ions and coordination complexes as novel carbapenem adjuvants. Antimicrob. Agents Chemother. 62 e02280-17.

Ferousi, C., Lindhoud, S., Baymann, F., Hester, E.R., Reimann, J., Karta, B., 2019. Discovery of a functional, contracted heme-binding motif within a multiheme cytochrome. J. Biol. Chem. 294 (45) https://doi.org/10.1074/jbc.RA119.010568.

Galili, T., O'Callaghan, A., Sidi, J., Sievert, C., 2018. Heatmaply: an R package for creating interactive cluster heatmaps for online publishing. Bioinformatics 34 (9), 1600–1602. https://doi.org/10.1093/bioinformatics/btx657.

Izadi, P., Izadi, P., Eldyasti, A., 2021. Holistic insights into extracellular polymeric substance (EPS) in anammosx bacterial matrix and the potential sustainable biopolymer recovery: A review. Chemosphere 274, 129703. https://doi.org/10.1016/j.chemosphere.2021.129703.

Kartal, B., Keltjens, J.T., 2016. Anammox Biochemistry: a Tale of Heme c Proteins. In Trends in Biochemical Sciences (Vol. 41, Issue 12). https://doi.org/10.1016/j.tibs.2016.08.015.

Kartal, B., van Niftrik, L., Keltjens, J.T., Huub, J.M., den Camp, Op, Jetten, M.S.M., 2012. Chapter 3 – Anammox - growth physiology, cell biology, and metabolism, editor Robert K. Poole, advances in microbial physiology. Academic Press 60, 211–262. https://doi.org/10.1016/B978-0-12-398264-3.00003-6.

Kartal, B., De Almeida, N.M., Maalcke, W.J., Op den Camp, H.J., Jetten, M.S., Keltjens, J. T., 2013. How to make a living from anaerobic ammonium oxidation. FEMS Microbiol Rev. May 37 (3), 428–461. https://doi.org/10.1111/1574-6976.12014. Epub 2013 Jan 21. PMID: 23210799.

Kartal, W.J., Maalcke, N.M., Almeida, De, Cirpus, J., Gloerich, W., Geerts, H.J., Op den Camp, H.R., Harhangi, E.M. Janssen, Megens, K.J., Francoijs, H.G., Stunnenberg, J. T., Keltjens, M.S. Jetten, Strous, M., 2011. Molecular mechanism of anaerobic ammonium oxidation. Nature 479, 127–130.

Kennes-Veiga, D.M., Trueba-Santiso, A., Gallardo-Garay, V., Balboa, S., Carballa, M., Lema, J.M., 2022. Sulfamethoxazole enhances specific enzymatic activities under aerobic heterotrophic conditions: a metaproteomic approach. Environ. Sci. Technol. 56, 13152.

Kuenen, J., 2008. Anammox bacteria: from discovery to application. Nat. Rev. Microbiol. 6, 320–326. https://doi.org/10.1038/nrmicro1857.

Ladomersky, E., Petris, M.J., 2015. Copper tolerance and virulence in bacteria. Metallomics 7 (6), 957–964. https://doi.org/10.1039/C4MT00327F.

Lawson, C.E., Nuijten, G.H.L., De Graaf, R.M., et al., 2021. Autotrophic and mixotrophic metabolism of an anammox bacterium revealed by in vivo ^{13}C and ^{2}H metabolic network mapping. ISME J. 15, 673–687. https://doi.org/10.1038/s41396-020-00805-w.

Li, G., Puyol, D., Carvajal-Arroyo, J.M., Sierra-Alvarez, R., Field, J.A., 2015. Inhibition of anaerobic ammonium oxidation by heavy metals. J. Chem. Technol. Biotechnol. 90, 830–837. https://doi.org/10.1002/jctb.4377.

Li, G.F., Ma, W.J., Cheng, Y.F., Li, S.T., Zhao, J.W., Li, J.P., Liu, Q., Fan, N.S., Huang, B. C., Jin, R.C., 2020. A spectra metrology insight into the binding characteristics of Cu2+ onto anammox extracellular polymeric substances. Chem. Eng. J. 393 https://doi.org/10.1016/j.cej.2020.124800.

Li, H., Yao, H., Zhang, D., Zuo, L., Ren, J., Ma, J., Pei, J., Xu, Y., Yang, C., 2018b. Short- and long-term effects of manganese, zinc and copper ions on nitrogen removal in nitritation-anammox process. Chemosphere 193, 479–488.

Li, J., Li, J., Gao, R., Wang, M., Yang, L., Wang, X., Zhang, L., Peng, Y., 2018a. A critical review of one-stage anammox processes for treating industrial wastewater: optimization strategies based on key functional microorganisms. Bioresour. Technol. 265 (498–505), 0960–8524. https://doi.org/10.1016/j.biortech.2018.07.013.

Luo, Qian, Fu, Liu, Zhang, Huang, Zhang., 2022. Responses of anammox to long-term p-nitrophenol stress: from apparent and microscopic phenomena to mechanism simulation. Bioresour. Technol. 355 (2022), 127265 https://doi.org/10.1016/j.biortech.2022.127265.

Ma, H., Zhang, Y., Xue, Y., Zhang, Y., Li, Y.-Y., 2019. Relationship of heme c, nitrogen loading capacity and temperature in anammox reactor. Sci. Total Environ. 659, 568–577. https://doi.org/10.1016/j.scitotenv.2018.12.377.

Madeira, C.L., De Araújo, J.C., 2021. Inhibition of anammox activity by municipal and industrial wastewater pollutants: a review. Sci. Total Environ. 799, 0048–9697. https://doi.org/10.1016/j.scitotenv.2021.149449.

Mesuere, B., Debyser, G., Aerts, M., Devreese, B., Vandamme, P., Dawyndt, P., 2015. The Unipept metaproteomics analysis pipeline. Proteomics 15, 1437–1442. https://doi.org/10.1002/pmic.201400361.

Morales, N., Val del Río, A., Vázquez-Padín, J.R., Gutiérrez, R., Fernández-González, R., Icaran, P., Rogalla, F., Campos, J.L., Méndez, R., Mosquera-Corral, A., 2015. Influence of dissolved oxygen concentration on the start-up of the anammox-based process: ELAN®. Water Sci. Technol. 72 (4), 520–527. https://doi.org/10.2166/wst.2015.233. PMID: 26247749.

More, T.T., Yadav, J.S.S., Yan, S., Tyagi, R.D., Surampalli, R.D., 2014. Extracellular polymeric substances of bacteria and their potential environmental applications. J. Environ. Manag. 144 (2014), 1–25. https://doi.org/10.1016/j.jenvman.2014.05.010.

Oliveros, J.C., 2007-2015. Venny. An interactive tool for comparing lists with Venn's diagrams. https://bioinfogp.cnb.csic.es/tools/venny/index.html.

Page, M.I., Badarau, A., 2008. The mechanisms of catalysis by metallo beta-lactamases. Bioinorg. Chem. Appl. 576297 https://doi.org/10.1155/2008/576297.

Pagliaccia, B., Carretti, E., Severi, M., Berti, D., Lubello, C., Lotti, T. (2022). Heavy metal biosorption by extracellular polymeric substances (EPS) recovered from anammox granular sludge, J. Hazard. Mater., Volume 424, Part C, 126661, doi:https://doi.org/10.1016/j.jhazmat.2021.126661.

Poulsen, J.S., Trueba-Santiso, A., Lema, J.M., Echers, S.G., Wimmer, R., Nielsen, J.L., 2023. Assessing labelled carbon assimilation from poly butylene adipate-co-terephthalate (PBAT) monomers during thermophilic anaerobic digestion. Bioresour. Technol. 385 (129430), 0960–8524. https://doi.org/10.1016/j.biortech.2023.129430.

Quiton-Tapia, S., Trueba-Santiso, A., Garrido, J.M., Suárez, S., Omil, F., 2023. Metalloenzymes play major roles to achieve high-rate nitrogen removal in N-damo communities: lessons from metaproteomics. Bioresour. Technol. 129476, 0960–8524. https://doi.org/10.1016/j.biortech.2023.129476.

Reimann, J., Jetten, M.S.M., Keltjens, J.T., 2015. Metal enzymes in "impossible" microorganisms catalyzing the anaerobic oxidation of ammonium and methane. Met. Ions Life Sci. https://doi.org/10.1007/978-3-319-12415-5_7.

Reino, C., Suárez-Ojeda, M.E., Pérez, J., Carrera, J., 2018. Stable long-term operation of an upflow anammox sludge bed reactor at mainstream conditions. Water Res. 128, 331–340. https://doi.org/10.1016/j.watres.2017.10.058.

Ren, Y., Hao Ngo, H., Guo, W., Wang, D., Peng, L., Ni, B.J., Wei, W., Liu, Y., 2020. New perspectives on microbial communities and biological nitrogen removal processes in wastewater treatment systems. Bioresour. Technol. 297, 122491 https://doi.org/10.1016/j.biortech.2019.122491.

Ren, Z.-Q., Wang, H., Zhang, L.-G., Du, X.-N., Huang, B.-C., Jin, R.C., 2022. A review of anammox-based nitrogen removal technology: from microbial diversity to engineering applications. Bioresour. Technol. 363 (127896), 0960–8524. https://doi.org/10.1016/j.biortech.2022.127896.

Strous, M., Heijnen, J.J., Kuenen, J.G., Jetten, M.S.M., 1998. The sequencing batch reactor as a powerful tool for the study of slowly growing anaerobic ammonium-oxidizing microorganisms. Appl. Microbiol. Biotechnol. 50, 589–596. https://doi.org/10.1007/s002530051340.

United Nations, 2015. Transforming our world: The 2030 agenda for sustainable development. A/RES/70/1. https://www.undp.org/sustainable-development-goals.

Val del Río, Á., da Silva, T., Martins, T.H., Foresti, E., Campos, J.L., Méndez, R., Mosquera-Corral, A., 2017. Partial Nitritation-Anammox granules: short-term inhibitory effects of seven metals on Anammox activity. Water Air Soil Pollut. 228, 439. https://doi.org/10.1007/s11270-017-3628-6.

Van de Graaf, A.A., de Bruijn, P., Robertson, L.A., Jetten, M.S.M., Kuenen, J.G., 1996. Autotrophic growth of anaerobic ammonium-oxidizing micro-organisms in a fluidized bed reactor. Microbiology (N Y) 142, 2187–2196. https://doi.org/10.1099/13500872-142-8-2187.

Wang, S., Ishii, K., Yu, H., Shi, X., Smets, B.F., Palomo, A., Zuo, J., 2021. Stable nitrogen removal by anammox process after rapid temperature drops: insights from metagenomics and metaproteomics. Bioresour. Technol. 320, 124231 https://doi.org/10.1016/j.biortech.2020.124231.

Wu, D., Li, G.F., Shi, Z.J., Zhang, Quan, Huang, Bao-Cheng, Fan, Nian-Si, Jin, Ren-Cun, 2019. Co-inhibition of salinity and Ni(II) in the anammox-UASB reactor. Sci. Total Environ. 669, 70–82. https://doi.org/10.1016/j.scitotenv.2019.03.130.

Yang, G.-F., Ni, W.-M., Wu, K., Wang, H., Yang, B.-E., Jia, X.Y., Jin, R.C., 2013. The effect of Cu (II) stress on the activity, performance and recovery on the anaerobic ammonium-oxidizing (Anammox) process. Chem. Eng. J. 226, 39–45.

Yang, Y., Li, M., Li, X.-Y., Gu, J.-D., 2018. Two identical copies of the hydrazine synthase gene clusters found in the genomes of anammox bacteria. Int. Biodeterior. Biodegrad. 132, 236–240.

Zhang, Y., Fonslow, B.R., Shan, B., Baek, M.C., Yates, J.R., 2013. Protein analysis by shotgun/bottom-up proteomics. Chem. Rev. 113, 2343–2394. https://doi.org/10.1021/CR3003533.

Zhang, Y.-Q., Sun, Q., Zhao, B.H., Li, J., Zhang, X.-Y., Zhang, B.L., Liu, B.J., 2023. Response of anammox to long-term stress of Ni(II): nitrogen removal, microbial products and microbial community. Biochem. Eng. J. 200, 109112 https://doi.org/10.1016/j.bej.2023.109112.

Zhang, Z.-Z., Deng, R., Cheng, Y.-F., Zhou, Y.-H., Buayi, X., Zhang, X., Wang, H.-Z., Jin, R.C., 2015. Behavior and fate of copper ions in an anammox granular sludge reactor and strategies for remediation. J. Hazard. Mater. 300, 838–846. https://doi.org/10.1016/j.jhazmat.2015.08.024.

Zhang, Z.-Z., Zhang, Q.-Q., Xu, J.-J., Deng, R., Ji, Z.-Q., Wu, Y.-H., Jin, R.-C., 2016. Evaluation of the inhibitory effects of heavy metals on anammox activity: a batch test study. Bioresour. Technol. 200, 208–216. https://doi.org/10.1016/j.biortech.2015.10.035.

Zhang, Z.-Z., Hu, H.-Y., Xu, J.-J., Shi, Z.-J., Shen, Y.-Y., Shi, M.-L., Jin, R.-C., 2017. Susceptibility, resistance and resilience of anammox biomass to nanoscale copper stress. Bioresour. Technol. 241, 35–43. https://doi.org/10.1016/j.biortech.2017.05.069.

Zhang, Z.-Z., Cheng, Y.-F., Xu, L.-Z.-J., Wu, J., Bai, Y.-H., Xu, J.-J., Shi, Z.-J., Jin, R.-C., 2018. Discrepant effects of metal and metal oxide nanoparticles on anammox sludge properties: a comparison between cu and CuO nanoparticles. Bioresour. Technol. 266, 507–515. https://doi.org/10.1016/j.biortech.2018.06.094.

Zhao, Y., Lin, Y.H., 2010. Whole-cell protein identification using the concept of unique peptides. Genomics Proteomics Bioinformatics 8, 33–41. https://doi.org/10.1016/S1672-0229(10)60004-6.

Zorz, J.K., Kozlowski, J.A., Stein, L.Y., Strous, M., Kleiner, M., 2018. Comparative proteomics of three species of Ammonia-oxidizing Bacteria. Front. Microbiol. 9 https://doi.org/10.3389/fmicb.2018.00938.